

Simulation of the oxidative metabolism of diclofenac by electrochemistry/(liquid chromatography/mass spectrometry)

Helene Faber · Daniel Melles · Christine Brauckmann ·
Christoph Alexander Wehe · Kristina Wentker ·
Uwe Karst

Received: 19 October 2011 / Revised: 7 December 2011 / Accepted: 15 December 2011 / Published online: 9 January 2012
© Springer-Verlag 2012

Abstract Diclofenac is a frequently prescribed drug for rheumatic diseases and muscle pain. In rare cases, it may be associated with a severe hepatotoxicity. In literature, it is discussed whether this toxicity is related to the oxidative phase I metabolism, resulting in electrophilic quinone imines, which can subsequently react with nucleophiles present in the liver in form of glutathione or proteins. In this work, electrochemistry coupled to mass spectrometry is used as a tool for the simulation of the oxidative pathway of diclofenac. Using this purely instrumental approach, diclofenac was oxidized in a thin layer cell equipped with a boron doped diamond working electrode. Sum formulae of generated oxidation products were calculated based on accurate mass measurements with deviations below 2 ppm. Quinone imines from diclofenac were detected using this approach. It could be shown for the first time that these quinone imines do not react with glutathione exclusively but also with larger molecules such as the model protein β -lactoglobulin A. A tryptic digest of the generated drug–protein adduct confirms that the protein is modified at the only free thiol-containing peptide. This simple and purely instrumental set-up offers the possibility of generating reactive metabolites of diclofenac and to assess their reactivity rapidly and easily.

Keywords Diclofenac · Electrochemistry · Phase I metabolism · Protein adducts · Glutathione adducts · High-resolution mass spectrometry

Published in the special paper collection on *Electrochemistry–Mass Spectrometry* with guest editors Uwe Karst and Martin Vogel.

H. Faber · D. Melles · C. Brauckmann · C. A. Wehe · K. Wentker ·
U. Karst (✉)
Institut für Anorganische und Analytische Chemie,
Westfälische Wilhelms-Universität Münster,
Corrensstraße 30,
48149 Münster, Germany
e-mail: uk@uni-muenster.de

Introduction

Diclofenac (DCI) is a non-steroidal, anti-inflammatory drug, which is frequently prescribed in the case of rheumatic diseases. However, toxic side effects may occur after administration of this drug, ranging from mild hematological responses in an uptake of certain aminotransferase levels to rarely observed severe necrotic liver injury [1]. Studies with ^{14}C -labeled DCI reveal that in humans DCI is almost completely metabolized and only little unmodified DCI is found either in urine or bile [2]. In fact, the bioactivation of DCI occurs via glucuronidation or oxidative metabolism [3], whereby both pathways result in reactive species. Therefore, the reason of this occasionally severe liver damage might be attributed to its metabolic conversion to reactive species. The formed metabolites may bind covalently to proteins, thus either leading to a disruption of critical cellular functions or to an immunological response.

Pumford et al. treated mice with DCI and were able to detect liver protein adducts of four different sizes (50, 70, 110, and 140 kDa) with a polyclonal antibody [4], but as their developed antibody was raised against acyl conjugates of DCI, the detected adducts presumably originated from the DCI acyl glucuronide. On the other hand, the 50 kDa protein adduct was later identified as a protein of microsomal origin. Furthermore, its formation appeared to be dependent on nicotinamide adenine dinucleotide phosphate (NADPH), thus implying a role of CYP enzymes in the previous bioactivation [5]. Shen et al. classified this protein as metabolizing cytochrome P450C11, clearly revealing that oxidative bioactivation leads to the formation of a highly reactive metabolite, which covalently modifies the enzyme and leads to its inhibition [6]. In human liver microsomes, the extent of protein modification is dependent on the activity of the phase I enzyme CYP3A4 involved in the biotransformation of DCI to 5-hydroxy-DCI (5-OH-DCI). Therefore, the oxidative

bioactivation seems to play an important role in the toxicity mechanism [7]. The 5-OH-DCI is also known to be a minor product formed *in vivo* and *in vitro* [8], but to be more reactive than its 4-hydroxylated isomer. Therefore, it is suspected to be primarily responsible for liver toxicity [7].

Besides, there is no clear correlation between the covalent modification of proteins by the acyl glucuronide of DCI and the hepatotoxicity. It was observed in rat hepatocytes that if the glucuronidation reaction is hindered by adding chemical inhibitors, the extent of covalent modification decreases, whereas the cytotoxicity increases [3]. Thus, the modification of proteins through glucuronides does not seem to be the key aspect in liver toxicity.

This finding correlates with the fact that an inhibition of CYP enzymes in rat hepatocytes results in a reduced cytotoxicity although, interestingly, the extent of covalent protein modification remains the same, presumably due to formation of acyl glucuronides [9, 10]. However, the reactivity towards proteins in complex samples such as *in vitro* assays or *in vivo* studies remains elusive, as reactive metabolites could react with many proteins present in the samples. The detection of such protein adducts in *in vitro* and *in vivo* approaches is difficult, time-consuming and requires the application of diverse analytical techniques such as chromatographic or electrophoretic separations, just to name a few [11].

In order to assess the reactivity of drug metabolites originating from oxidative metabolism, a rapid and easy method would be useful. In recent years, the simulation of phase I metabolism using electrochemistry has gained more attention. It was shown by Bruins and coworkers that certain reactions, which are initiated by a single electron transfer, are readily simulated by direct electrochemical oxidation, in particular aromatic hydroxylation, S- and P-oxidation, N-dealkylation and dehydrogenation reactions. Electrochemistry (EC) is not capable of mimicking reactions which require the initial abstraction of protons, including aliphatic hydroxylation, N-oxidation, O-dealkylation, and hydroxylation of unsubstituted aromatic compounds [12]. Several reviews deal with the potential and limitations of this technique, influences on the cell design and further technical developments, including the miniaturization of this approach [13–17]. With respect to the investigation of drug–protein adducts, Lohmann et al. applied EC/LC-MS to generate reactive phase I metabolites of the drugs acetaminophen, amodiaquine, and clozapine, which were further allowed to react with a model protein (β -lactoglobulin A) and human serum albumin, thus generating enough drug–protein adducts for further investigations [18]. The major advantage of this purely instrumental approach is the absence of a biological matrix. Hence, reactions with certain proteins of interest can be studied.

In previous work by Madsen et al., diclofenac was oxidized electrochemically in a coulometric flow through cell

[19]. In this work, 5-OH-DCI and the corresponding quinone imine could be generated. The authors demonstrated that these electrophilic species can react with glutathione to form different adducts. Based on the instrumental approach, they could develop a sensitive method for the detection of adducts in *in vitro* and *in vivo* samples. However, no information exists about a possible reaction of the formed reactive metabolites with larger biomolecules. Therefore, it is of strong interest to investigate the potential of reactive metabolites, especially the quinone imine of 5-OH-DCI, to bind covalently to proteins. The respective work is described in this manuscript.

Experimental

Chemicals

DCI, glutathione (GSH), β -lactoglobulin A (LGA), ammonium acetate (NH_4 acetate), acetaminophen (APAP), urea, tris(2-carboxyethyl)phosphine hydrochloride (TCEP) and trypsin from bovine pancreas were obtained from Sigma Aldrich (Steinheim, Germany). Formic acid was purchased from Fluka Chemie (Buchs, Switzerland). Water was purified prior to its use with an Aquatron A4000D system (Barloworld Scientific, Nemours Cedex, France). Acetonitrile (ACN) was obtained from Merck (Darmstadt, Germany) and was of gradient grade. The other chemicals were of the highest quality available. For desalting the protein samples, PD-10 Sephadex desalting columns were used (GE Healthcare, Buckinghamshire, U.K.).

Electrochemical oxidation and mass spectrometric detection

DCI (50 μM in 5 mM NH_4 acetate (pH 7.4)/ACN 50/50 *v/v*) was oxidized in a thin layer cell equipped with a boron doped diamond working electrode (Antec Leyden, Zoeterwoude, The Netherlands). The potential of the cell was controlled either by a Roxy potentiostat (Antec Leyden) or by a homemade device. In order to obtain a quick overview over the oxidation products, a mass voltammogram of DCI was recorded. For this purpose, DCI was pumped through the cell at a flow rate of 10 $\mu\text{l}/\text{min}$ by a syringe pump (model 74900 from Cole Parmer, Vernon Hills, IL, USA) and the potential was ramped from 0 to 2.5 V within 250 s. The outlet of the electrochemical cell was coupled to an orbitrap mass spectrometer (Exactive, Thermo Fisher Scientific, Bremen, Germany), operated in negative ion mode. The obtained mass spectra are displayed in a three-dimensional plot, depending on the applied voltage. The mass spectrometric parameters for the orbitrap were: scan range m/z 120.0–1,600.0; HCD gas, on; resolution, high; polarity negative; microscans, 1; AGC target, balanced; maximum inject time, 100 ms; sheath gas flow rate, 10 a.u.; aux gas and sweep gas flow rate, 0; spray voltage, 3.20 kV; capillary temp., 275 $^\circ\text{C}$;

capillary voltage, -60.00 V; tube lens voltage, -65.00 V; skimmer voltage, -18.00 V.

Chromatographic separation and mass spectrometric detection of oxidation products and glutathione adducts

In order to obtain more information about the oxidation products and to separate the glutathione adducts, a chromatographic separation was carried out. DCI was oxidized at a potential of 2.4 V, which was selected due to the optimum potential in the mass voltammogram, assuring the optimum yield of oxidation products. The effluent of the electrochemical cell was collected in a vial containing 5 mM NH_4 acetate or, in case of adduct formation experiments, 1 mM GSH dissolved in NH_4 acetate. Subsequently, 5 μL of this mixture were injected into the HPLC-MS system consisting of an autosampler and an Accela 600 HPLC pump, a RP18 column (Hypersil Gold, 150×2.1 mm, 3 μm particle size) and an Exactive orbitrap mass analyzer (all from Thermo Fisher Scientific, Bremen, Germany). The eluents used for the separation were 10 mM NH_4 acetate (pH 7.4) and acetonitrile. The flow rate was 300 $\mu\text{L}/\text{min}$ and the gradient profile is shown in Table 1. The mass spectrometric parameters were: scan range from m/z 120 to $1,600$; HCD gas, on; resolution, high; polarity, negative; microscans, 1 ; AGC Target, balanced; maximum inject time, 100 ms; sheath gas flow rate, 40 a.u.; aux gas flow rate, 10 a.u.; sweep gas flow rate, 0 a.u.; spray voltage, 4.00 kV; capillary temp., 325 $^\circ\text{C}$; capillary voltage, -32.50 V; tube lens voltage, -100.00 V; skimmer voltage, -18.00 V.

For fragmentation with the orbitrap mass spectrometer, two different options were used: on the one hand, the higher-energy collisional dissociation (HCD) was used at different energies (15.0 , 20.0 , and 25.0 eV) and on the other hand, the fragmentation was performed by using collision-induced dissociation at 25.0 eV.

Adduct formation with β -lactoglobulin A and tryptic digest

A solution of DCI (0.2 mM in 5 mM NH_4 acetate (pH 7.4)/ACN $50/50$ v/v) was oxidized at an optimum potential of 2.4 V and the effluent of the electrochemical cell was conducted into a vial containing LGA (dissolved in water, heated up at 95 $^\circ\text{C}$ for 5 min prior to its use) at a concentration of 0.02 mM. After 15 min the mixture was separated on a C5 Wide Pore Column (Discovery BIO Wide Pore C5, 150×2.1 mm, 5 μm particle size, Supelco, Steinheim, Germany)

in order to remove the excess of native DCI. The eluents used were 0.1% FA (pH 2.6) and ACN and the flow rate was 300 $\mu\text{L}/\text{min}$. The corresponding gradient profile is shown below in Table 2. The HPLC system used was from Antec Leyden and comprised two LC 100 pumps, an OR 110 organizer rack with a degasser and a pulse dampener, an AS 100 autosampler and a Roxy potentiostat and column oven. The time-of-flight mass spectrometer was from Bruker Daltonics (model microToF MS, Bremen, Germany) and the mass spectrometric parameters used were: ESI(+); nebulizer (N_2), 1.8 bar; dry gas (N_2), 8.0 l/min; dry temperature, 190 $^\circ\text{C}$; capillary, -4.0 kV; endplate offset, -300 V; capillary exit, 180.0 V; skimmer 1, 60.0 V; skimmer 2, 22.5 V; hexapole 1, 25.0 V; hexapole RF, 450 V; lens transfer time, 60.0 μs ; pre pulse storage time, 15.0 μs ; lens 1 storage, 30.0 V; lens 1 extraction, 20.3 V; lens 2, 7.4 V; lens 3, 21.0 V; lens 4, 0.3 V; lens 5, -27.5 V; mass to charge (m/z) ratio range, 300 – $3,000$. For tryptic digest, the drug–protein adducts were generated by oxidizing DCI (0.5 mM in NH_4 acetate/ACN, $50/50$, v/v) at 2.4 V for 100 min and collecting this solution in a vial containing 1 ml of 0.1 mM LGA dissolved in 8 M urea. The excess of salts and unoxidized DCI were removed on a PD-10-Sephadex desalting column according to the supplier's protocol. Subsequently, the disulfide bridges were reduced by adding a solution of 100 mM TCEP (in 0.3 M ammonia) to the drug–protein adduct, in particular, a ninefold molar excess of TCEP per oxidized S-atom in LGA. After removal of the reagent through another desalting column, 50 mM ammonium bicarbonate and 5 μL trypsin (2.3 mg dissolved in 1 ml water) were added. After 90 min of incubation, the tryptic digest was stopped by adding 200 μL ACN containing 1% FA. The mixture was analyzed by the HPLC-ToF-MS system mentioned previously.

Results and discussion

Electrochemical oxidation of diclofenac

First, a mass voltammogram was recorded for DCI in order to obtain a rapid overview about oxidation products and to define the optimum potential for further conjugation experiments. The obtained three-dimensional plot is shown in Fig. 1. DCI was detected as $[\text{M}-\text{H}]^-$ ion at m/z 294 and as decarboxylation product at m/z 250 due to degradation in the interface. With increasing potential, it is obvious that the m/z ratios of DCI and decarboxylated DCI are decreasing in

Table 1 Gradient profile used for the chromatographic separation of oxidation products

Time [min]	1 min	2 min	8 min	11 min	12 min	13 min	20 min
Concentration ACN (Eluent B)	10%	20%	50%	80%	80%	10%	Stop

Table 2 Gradient profile used for the chromatographic separation of protein adducts and their peptides after tryptic digest

Time [min]	2 min	6 min	9 min	12 min	15 min
Concentration ACN (Eluent B)	25%	65%	65%	25%	Stop

intensity, starting approximately at 1,000 mV vs Pd/H₂. In contrast to that other signals with *m/z* ratios of 264, 280, 282, 310, 324, and 326 increase, indicating electrochemical oxidation. Using a high-resolution mass spectrometer, it is possible to receive sum formulae for the oxidation products. An overview over the calculated sum formulae and the respective deviation between measured and calculated mass is presented in Table 3. Based on these sum formulae, structures were proposed which are depicted in Fig. 2. DCI is oxidized to a +O product at *m/z* 310 (P-1, P-2, C₁₄H₁₀Cl₂NO₃, 0.07 ppm). This is presumably OH-DCI, as formerly described by Madsen et al. [19]. The *m/z* ratio at 266 is presumably formed during fragmentation in the electrospray interface (decarboxylation resulting in C₁₃H₁₀Cl₂NO, 0.37 ppm).

The *m/z* ratio of 264 can be assigned to the molecular formula of C₁₃H₈Cl₂NO, (1.16 ppm). As this *m/z* ratio is 2 amu lower than 266, it could be assumed that it originates from a decarboxylation of *m/z* 308 (P-3), the corresponding quinone imine of *m/z* 310, yet no increasing signal at *m/z* 308 is observed in the mass voltammogram. The generation of an imine methide by electrochemical decarboxylation, corresponding to the sum formula of C₁₃H₈Cl₂NO, seems to be unlikely as well. Electrochemical decarboxylations are known for a long time as the Kolbe synthesis, but mostly they yield the dimeric product of the carboxylic acid substrates, depending on buffer, electrode, and temperature [20]. Other possible products generated during Kolbe

synthesis, for example alcohols or olefins, are rather regarded as byproducts. As no dimer originating from an intermediate decarboxylated radical is detectable, this reaction pathway seems unlikely. Electrochemically generated imine methides are described in literature for 3-methylindole or the antibiotic trimethoprim [21], although, when oxidized, the reactive imine methide is obtained from a simple dehydrogenation reaction, commonly known from electrochemical oxidations [12].

Besides, a further oxidation to a +2O product is observed at *m/z* 326 (P-4, C₁₄H₁₀Cl₂NO₄, 0.36 ppm). A dehydrogenation of *m/z* 326 leads to a product at *m/z* 324 (P-5, C₁₃H₈Cl₂NO₄, 0.02 ppm, see Fig. 2). These oxidation products have not been described previously. This could be attributed to the fact that in this work, boron doped diamond was used as working electrode material instead of glassy carbon. This working electrode allows to apply higher potentials of up to 2.5 V (vs. Pd/H₂) due to the higher overpotential for the anodic generation of oxygen. At higher potentials, it is likely that hydroxyl radicals are formed. They result in hydroxylation, which is not obtained with other electrode materials [22]. Furthermore, two signals at *m/z* 282 and *m/z* 280 are arising during oxidation. They could be assigned to a +2O product, which is subsequently decarboxylated (P-6, *m/z* 282, C₁₃H₁₀Cl₂NO₂, 1.15 ppm) and dehydrogenated (P-7, *m/z* 280, C₁₃H₈Cl₂NO₂, 1.40 ppm). Whether these signals originate from decarboxylation during electrospray ionization of *m/z* 326 (P-4) and 324 (P-5) or from the electrochemical oxidation, respectively, cannot be clarified without a chromatographic separation. Due to the fact that DCI contains two chlorine atoms, the isotopic pattern of the oxidation products will overlap, especially with the dehydrogenation product. The use of a high-resolution mass spectrometer, however, offers the opportunity to resolve the pattern by accurate mass measurements and to simplify their detection.

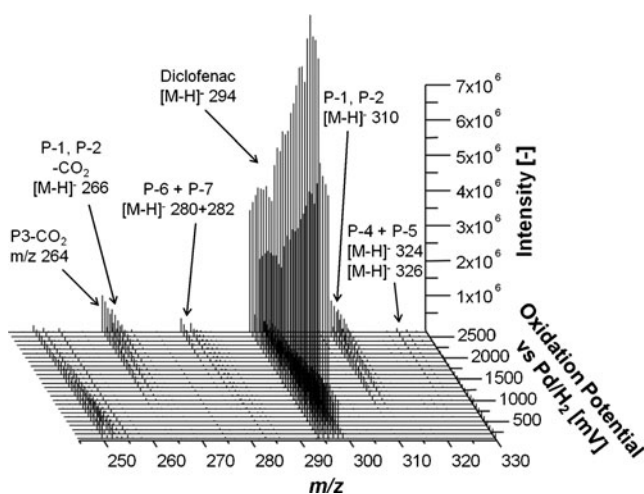


Fig. 1 Electrochemical oxidation of DCI and recorded mass voltammogram. The potential was ramped from 0–2.5 V with a scan rate of 10 mV/s and the mass spectra were plotted in dependency of the applied potential. DCI is visible as [M–H]⁺ ion at *m/z* 294

Chromatographic separation of oxidation products

In order to obtain more information about the polarity of the oxidation products and to gain more insight about structural properties by fragmentation, a chromatographic separation was established on a RP-column. Figure 3 (left side) displays a chromatogram obtained after oxidation of DCI at a potential of 2.4 V, which delivered the highest attainable yield of oxidation products. DCI is observed at an *m/z* ratio of 294 (9.70 min). The product with *m/z* 310 elutes earlier than the parent drug (7.78 min). This is in accordance to a

Table 3 Overview of products formed during electrochemical oxidation, proposed sum formulae and deviations between measured and calculated mass (derived from the mass voltammogram recorded with an orbitrap mass spectrometer)

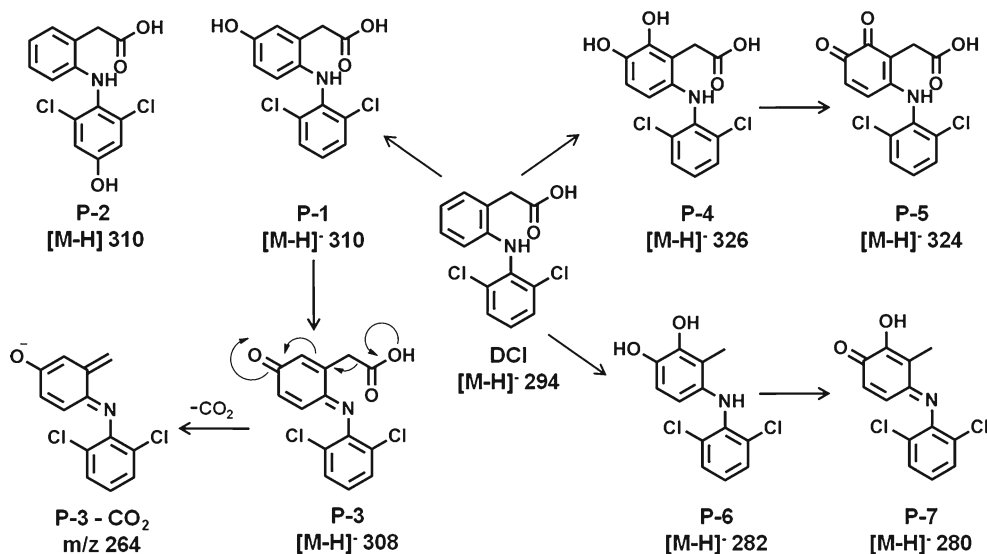
<i>m/z</i> measured	Abbreviation	Sum formula	<i>m/z</i> theoretical	Deviation (measured/calculated) [ppm]	
294.0095	DCI	DCI	[M-H] ⁻ =C ₁₄ H ₁₀ Cl ₂ NO ₂	294.0083	0.45
250.0197	DCI-CO ₂		[M-H] ⁻ =C ₁₃ H ₁₀ Cl ₂ N	250.0185	0.41
310.0043	DCI + O	P-1 P-2	[M-H] ⁻ =C ₁₄ H ₁₀ Cl ₂ NO ₃	310.0032	0.07
263.9991	DCI + O-CO ₂ -2H	P-3 -CO ₂	[M-H] ⁻ =C ₁₃ H ₈ Cl ₂ NO	263.9977	1.16
266.0146	DCI + O-CO ₂		[M-H] ⁻ =C ₁₃ H ₁₀ Cl ₂ NO	266.0145	0.37
325.9991	DCI + 2O	P-4	[M-H] ⁻ =C ₁₄ H ₁₀ Cl ₂ NO ₄	325.9981	0.36
323.9836	DCI + 2O-2H	P-5	[M-H] ⁻ =C ₁₄ H ₈ Cl ₂ NO ₄	323.9825	0.02
282.0098	DCI + O-CO ₂	P-6	[M-H] ⁻ =C ₁₃ H ₁₀ Cl ₂ NO ₂	282.0210	1.53
279.9942	DCI + O-CO ₂ -2H	P-7	[M-H] ⁻ =C ₁₃ H ₈ Cl ₂ NO ₂	279.9926	1.40

hydroxylation, which typically coincides with an increase in polarity. As formerly discussed by Madsen et al., the hydroxylation preferably takes place at the C5-position at the aromatic ring due to a steric hindrance at the 3-C' position and the electron withdrawing chlorine atoms, which hinder a hydroxylation at the 4'-C [19]. In vitro incubations with rat liver microsomes (RLM) with DCI and subsequent chromatographic separation reveal two hydroxylation products, in case of adding human liver microsomes (HLM) only one hydroxylated metabolite. As it is known that the 4'-hydroxylation is a major product in the enzymatically catalyzed oxidation [7], whereas EC will rather yield 5-OH-DCI [19], the other peak can be assigned to the 5-hydroxylated isomer (P-1).

The +2O product with *m/z* 326 (P-4) elutes even earlier than the +O product (6.66 min), which is due to the enhanced polarity as a result of the second hydroxyl group. For the second O-atom, it is not unequivocally clear, where the hydroxylation occurs. On the one hand, it is conceivable that due to the higher potential used here, hydroxyl radicals are generated, which attack non-preferred positions (C4').

On the other hand, it seems more likely that the oxidation will continue at the aromatic ring already bearing one hydroxyl group, as it is known that the activation of aromatic rings by a hydroxyl group results in further oxidation [12]. However, further reaction would presumably not stop at the catechol stage and would continue to yield the corresponding quinone, so that *m/z* 324 (P-5, 8.13 min) is likely to be assigned to the quinoid form of *m/z* 326 (P-4), resulting from dehydrogenation.

The oxidation product with *m/z* 282 (P-6) was formerly attributed to a +2O product, presumably originating from *m/z* 326 (P-4) by decarboxylation, but as they can be separated from each other, this cannot be a fragment arising in the electrospray source. It elutes later than DCI itself (9.95 min), which can be explained by the loss of the polar carboxylic moiety. Subsequently, the less polar dehydrogenation product at *m/z* 280 (P-7) elutes later than *m/z* 282 (11.28 min). The mechanism for the electrochemical generation of these decarboxylation products, however, remains elusive, as a mechanism similar to the Kolbe synthesis would involve the formation of dimers out of radical intermediates, which are

Fig. 2 Overview about electrochemically generated oxidation products of DCI and their proposed structures

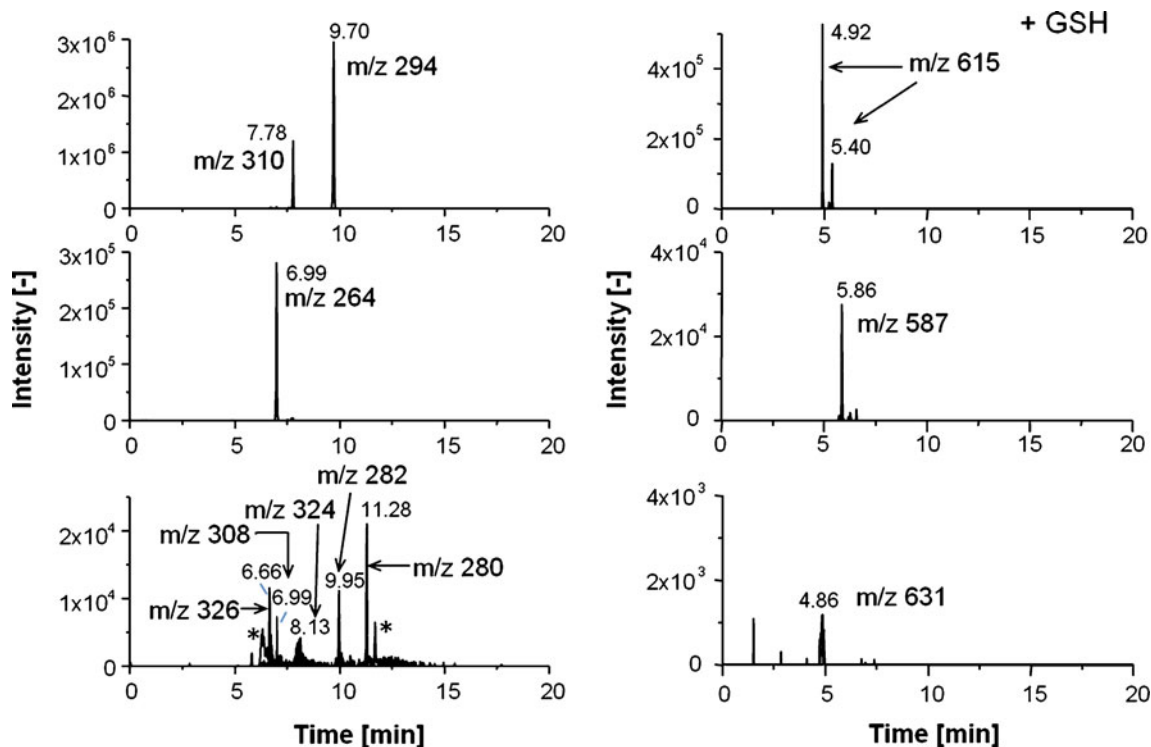


Fig. 3 Chromatographic separation of DCI, its oxidation products and glutathione adducts on a reversed phase column. DCI was oxidized at a constant potential of 2.4 V vs. built-in reference and the EC effluent was collected in a vial containing buffer or glutathione, respectively. Afterwards, the mixture was analyzed by HPLC/ESI-MS. *Left column* extracted ion chromatograms of DCI and its oxidation products (P-1 m/z 310, P-3 m/z

308, m/z 264 P-3-CO₂, P-4 m/z 326, P-5 m/z 324, P-6 m/z 282 and P-7 m/z 280). *Right column* extracted ion chromatograms of the four glutathione adducts with m/z 587, m/z 615, and m/z 631. The peaks marked with an asterisk originate from the m/z ratio of 280, but the isotopic pattern reveals that they contain no chlorine, thus they cannot be assigned to P-7

not observed at all. For m/z 264 (6.99 min), the sum formula C₁₃H₈ONCl₂ can be assigned with a deviation between measured and calculated mass of 0.47 ppm. Of all oxidation products, it shows the least retention, which would be unlikely if it originated from a decarboxylation. To elucidate the structure of the product, LC-MS/MS measurements have been carried out using HCD fragmentation. The MS/MS spectrum for the peak at 6.99 min displays fragments at m/z 228 (-HCl) and 192 (-2HCl). In comparison to this, the fragmentation of m/z 310 yields products at m/z 266 (-CO₂), 230 (-CO₂, -HCl) and 194 (-CO₂, -2HCl) (data not shown). The fragmentation patterns resemble each other, despite of the fact that in the case of the peak at 6.99 min, the fragments are always lighter by 2 amu. This supports the assumption that the peak at 6.99 min originates from m/z 308 (P-3), the quinone imine from OH-DCI. A closer look at the non-fragmented spectrum at 6.99 min reveals a small signal at m/z 307.9887, which can be assigned to the sum formula C₁₃H₈NO₃Cl₂ corresponding to the quinone imine with a deviation of 0.03 ppm between measured and calculated mass. The peak with m/z 308 coelutes with m/z 264. Thus, it is likely that after elution of the quinone imine, it decarboxylates during ionization yielding m/z 264, which gives a more intense ion signal than for the precursor ion. Furthermore, this peak completely disappears in presence of

glutathione within 1 h and corresponding glutathione adducts of the quinone imine are observed at m/z 615 (see section [Chromatographic separation of oxidation products](#)). Due to the use of a high-resolution mass spectrometer, it is possible to detect the quinone imine with high mass accuracy, whereas other instruments such as an ion trap mass spectrometer did not enable the detection of the quinone imine (data not shown). Furthermore, the use of a chromatographic separation proves to be essential in this case, as the intensity of m/z 308 (P-3) appeared to be too low in the mass voltammogram otherwise.

Formation of glutathione adducts

When DCI is oxidized electrochemically at 2.4 V and the effluent of the electrochemical cell is collected in a vial containing GSH, four different adducts emerge. Figure 3 (right side) displays the chromatographic separation after an incubation time of 1 h. At 4.92 and 5.40 min two GSH adducts with an m/z ratio of 615 elute, corresponding to the reaction of the above mentioned DCI quinone imine (m/z 308) with GSH (C₂₄H₂₅O₉N₄Cl₂S, 1.09 and 1.35 ppm, respectively). These findings confirm the results of Madsen et al. who have also found two isomeric adducts after direct

electrochemical oxidation of DCI and trapping with GSH [19]. A comparison with literature data concerning the incubation of 5-OH-DCI and rat liver microsomes also reveals two GSH conjugates [23], although incubations with RLM and HLM did not reveal GSH conjugation. This might be due to the low extent of 5-hydroxylation in microsomes or direct reaction with proteins from the biological matrix (data not shown). Additionally, two other adducts were found. The peak at 4.86 min can be assigned to m/z 631, a GSH adduct of the quinone imine of the dihydroxylated DCI mentioned above (P-5, m/z 324) with a sum formula of $C_{24}H_{25}O_{10}N_4Cl_2S$, (1.14 ppm). Due to the additional hydroxyl group, the adduct elutes prior to m/z 615. Interestingly, Madsen et al. were able to detect a GSH adduct derived from a dihydroxylated metabolite in rats (bile) dosed with DCI [19]. In this case, however, the structure of the adduct remains elusive, as the fragmentation delivers only little information. The GSH conjugate, which elutes at 5.86 min with m/z 587, results from reaction of P-6 (m/z 280) with GSH ($C_{23}H_{25}O_8N_4Cl_2S$, 0.30 ppm). This adduct elutes later than the others due to the loss of the polar carboxylic acid group. The fragment spectra of these adducts are depicted in Figs. 4, 5, and 6. The signals with m/z 128, 143, 179, 210, 254 and the most intense fragment at m/z 272 result from fragmentation of the GSH moiety and can be assigned to the commonly known fragmentation pattern of GSH [24]. For m/z 615 and 587, a cleavage adjacent to the thioether moiety occurs, which derives a fragment at 341.9 or 313.9 respectively. For the GSH adduct with m/z 631, such a fragment is not observed, only the loss of water and carbon dioxide and their sodium adducts are visible. In the HCD fragment spectrum of m/z 631, however, a fragment is detected at m/z 295.7 (see Fig. 6) which can be

assigned to a molecular formula of $C_{13}H_8ONCl_2S$ with a mass deviation of 0.16 ppm. This fragment presumably originates from a cleavage at the thioether moiety with a subsequent loss of water and carbon dioxide. To summarize, despite of these sulfur containing backbones, the fragmentation pattern does not provide a further understanding where the GSH moiety is located in the molecules, as the fragmentation mostly occurs within the GSH moiety and not in the backbone of the adducts. However, it can be shown that the electrochemically generated products show reactivity towards thiols. Therefore, it was of interest if they would show a reaction with thiol groups from larger molecules such as proteins.

Formation of protein adducts and tryptic digest

To elucidate the reactivity of the electrochemically generated products towards proteins, DCI was oxidized and the products were allowed to react with β -lactoglobulin A (β -LGA). In fact, β -LGA is the main whey protein in milk, but since this protein is of moderate size (162 amino acids, 18 kDa), it shows a structural homogeneity and is ionized easily in the electrospray source. As this protein bears one free thiol group within the T13 peptide, it is suitable to begin investigations of the reactivity of metabolites towards proteins, as it could already be shown in previous work for paracetamol, clozapine, and amodiaquine [18]. Figure 7 (top) displays the time-of-flight mass spectrum of β -LGA after reaction of DCI, which was oxidized previously at 2.4 V. The protein is visible at multiply charged states (left part in Fig. 7). A closer look at the different charge states reveals signals shifted towards higher m/z values. Therefore, a reaction of metabolites with the protein has presumably

Fig. 4 LC-MS/MS spectrum (HCD fragmentation, 25.0 eV) of the glutathione adduct with m/z 615. The smaller fragment spectrum shows the enlarged section from m/z 285–650

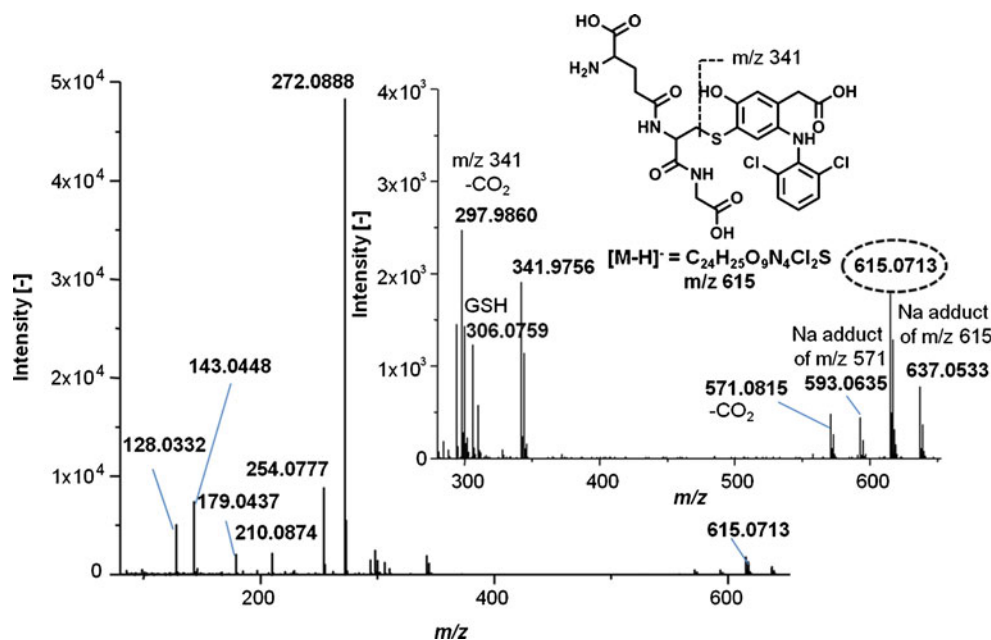
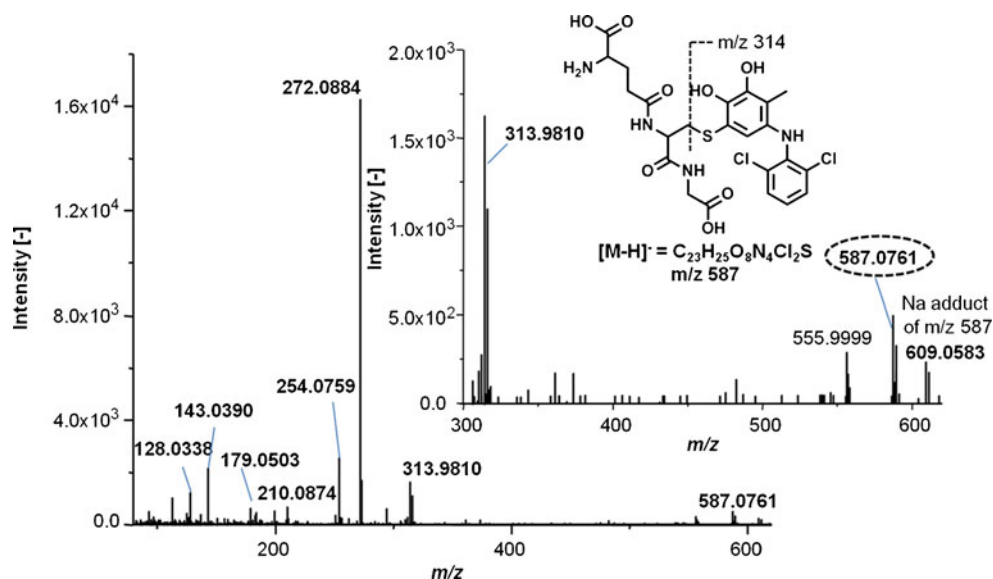


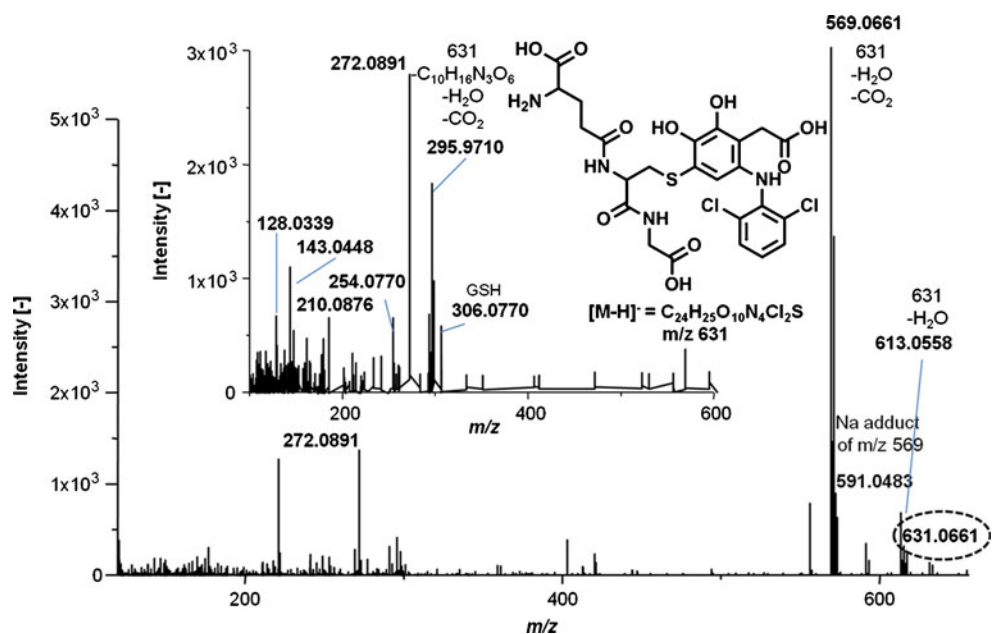
Fig. 5 LC-MS/MS spectrum (HCD fragmentation, 25.0 eV) of the glutathione adduct with m/z 587. The smaller fragment spectrum shows an enlarged view of the m/z range from 300–620



taken place, although a certain amount of unmodified protein is still left. A deconvolution of this spectrum results in the right spectrum, providing the neutral masses of the obtained adducts. Unmodified β -LGA was determined at a mass of 18,363 Da. Additional peaks are detected at neutral masses of 18,644, 18,673, and 18,687 Da respectively, corresponding to the addition of P-3, P-5, and P-7 to β -LGA. As these metabolites have shown a reaction with thiols such as GSH, as demonstrated above, they have presumably reacted with the accessible thiol moiety of the T13 peptide. In comparison to the reaction of DCI with β -LGA, a reaction with electrochemically generated *N*-acetyl-*p*-benzoquinone imine (NAPQI) from APAP with β -LGA was carried out as well. NAPQI is generated from APAP by dehydrogenation during electrochemical oxidation. As it is

known from previous work, it shows a high reactivity towards β -LGA and thiols in general due to its electrophilic structure [18] and was consequently selected as a positive control. Figure 7 (bottom) shows the time-of-flight mass spectra and the deconvolution results obtained for the reaction with β -LGA and NAPQI. In comparison to DCI, the amount of unmodified β -LGA is much lower, implicating a greater reactivity. However, no information is obtained regarding the amount of electrochemical generated products in case of APAP and DCI, rendering a direct comparison difficult. For DCI, the reaction with the specific T13 peptide remains to be investigated. In order to reveal a reaction with this thiol-containing peptide, a tryptic digest was carried out and the peptides were analyzed by LC-ToF-MS. In Fig. 8, the time-of-flight mass spectra after chromatographic

Fig. 6 LC-MS/MS spectrum (in source CID, 25.0 eV) of the glutathione adduct with m/z 631. The small section shows the HCD fragment spectrum (HCD, 25.0 eV)



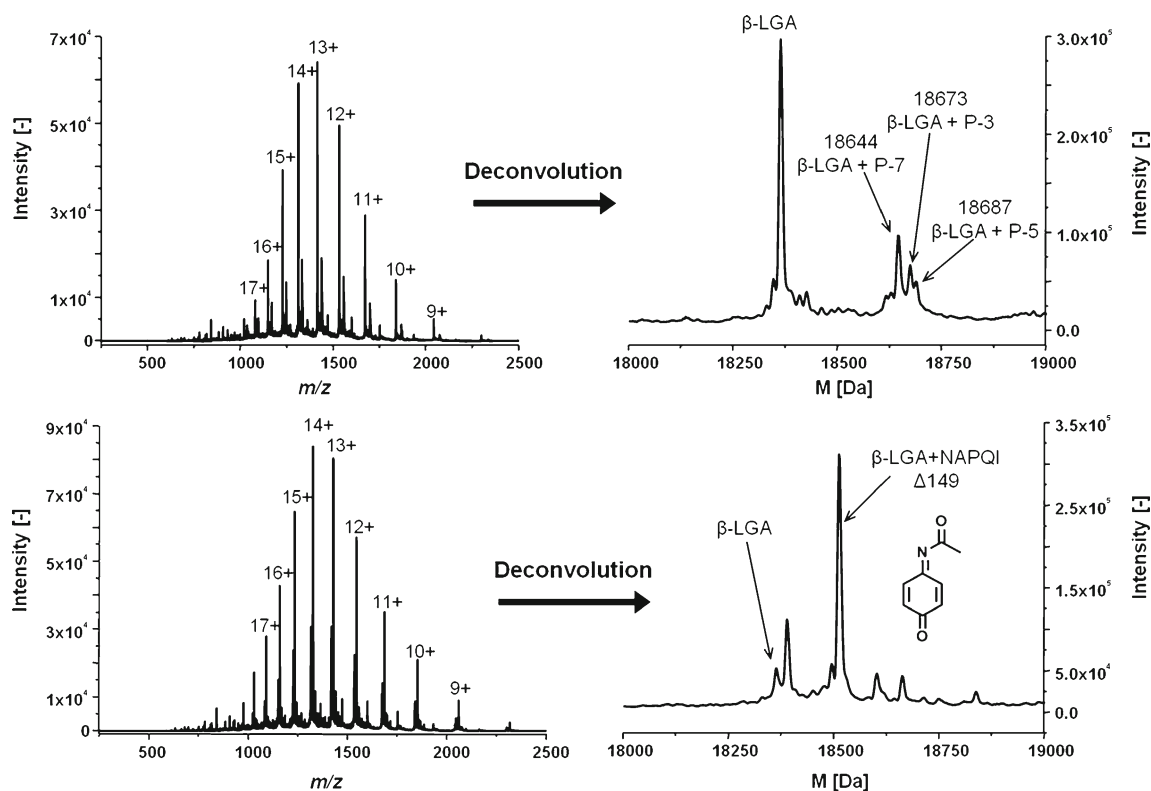


Fig. 7 Time-of-flight mass spectra and deconvolution results of modified β -LGA after incubation with a DCI solution oxidized electrochemically at 2.4 V (top) and acetaminophen oxidized at 1.5 V (bottom)

separation of the peptides are presented. The unmodified T13 peptide (left spectrum in Fig. 8) is detected at a m/z ratio of 1,337.1120 as doubly charged ion ($[M + 2H]^{2+} = C_{115}H_{183}N_{29}O_{36}S_4$, 0.45 ppm) and m/z 891.7488 as triply charged ion ($[M + 3H]^{3+} = C_{115}H_{184}N_{29}O_{36}S_4$, 5.16 ppm). The right spectrum shows the modified peptide. The reaction of β -LGA with P-3 results in a modification of the T13 peptide, observed at m/z 1,491.5995 and m/z 994.7419. These signals

correspond to $[T13 + P-3 + 2H]^{2+}$ and $[T13 + P-3 + 3H]^{3+}$ with a deviation of 7.44 ppm (doubly charged peptide $C_{129}H_{192}N_{30}O_{39}S_4Cl_2$) and 0.90 ppm (triply charged peptide $C_{129}H_{193}N_{30}O_{39}S_4Cl_2$) between measured and calculated mass. The signal at m/z 1,477.6060 and m/z 979.4013 can be traced back to a modification of T13 through P-7, resulting in $[T13 + P-7 + 2H]^{2+}$ ($C_{128}H_{192}N_{30}O_{38}S_4Cl_2$, 4.81 ppm) and $[T13 + P-7 - H_2O + 3H]^{3+}$ ($C_{128}H_{191}N_{30}O_{37}S_4Cl_2$, 6.53 ppm).

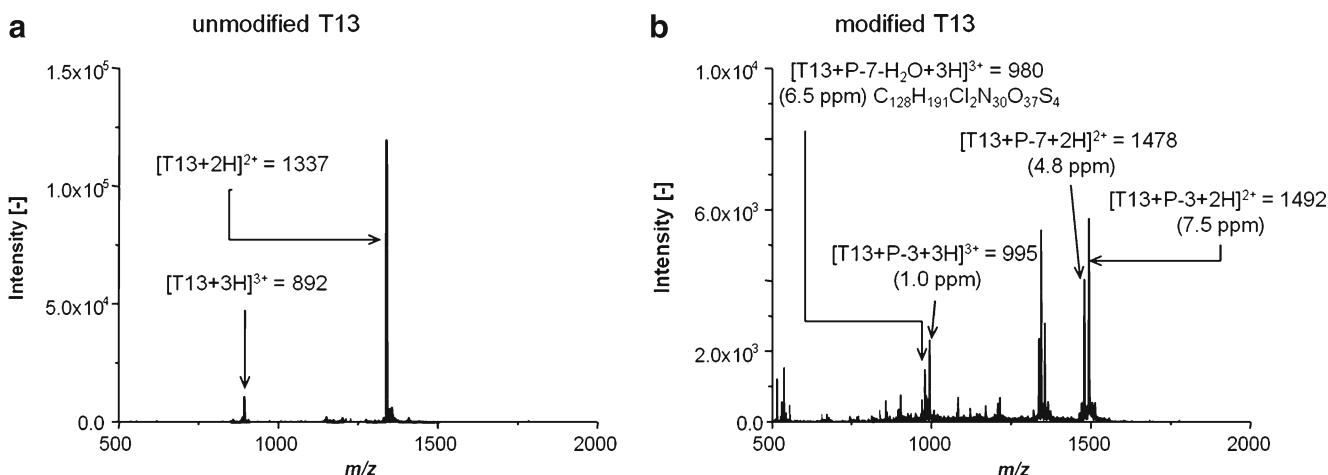


Fig. 8 Tryptic digest of β -lactoglobulin A modified with electrochemically generated oxidation products of DCI. Left time-of-flight mass spectrum of the thiol-containing T13 peptide of β -LGA (unmodified). Right corresponding mass spectrum of the modified T13 peptide

However, for the metabolite P-5, no modified T13 was detected. This metabolite is either likely to be generated only to a small extent during electrochemical oxidation or it only shows a minor reactivity towards the model protein, since the reaction with GSH yielded one adduct of minor intensity (see Fig. 3). It thus seems to be crucial to not only concentrate on the identification of the electrochemically generated products, but also on their quantification with the goal to allow a more precise assessment of their reactivity. Since internal standards are not always available, the quantification by means of inductively coupled plasma–mass spectrometry (ICP-MS) for heteroatom containing drugs like DCI seems to be of great interest and needs further investigations.

Conclusions

Electrogenerated oxidation products for DCI were prepared on boron doped diamond as working electrode material, as it allows to apply higher potentials and to identify more metabolites than in previous work. This is possibly due to the generation of hydroxyl radicals, which may attack non-preferred positions in the molecule. In combination with high-resolution mass spectrometry using either a time-of-flight mass spectrometer or an orbitrap mass spectrometer, the detection of oxidation products, especially with its characteristic chlorine isotope pattern, was simplified, as no overlap of isotope patterns was observed. The extension of the set-up by a chromatographic separation of oxidation products in combination with tandem mass spectrometry proved to be essential to distinguish between different possible structures.

The reactivity of the generated products was assessed by adding trapping reagents such as glutathione, resulting in four different adducts. Hereafter, the reactivity towards proteins was investigated, revealing a reaction with thiol-containing peptides of a model protein. Compared to already known reactions between the liver toxic metabolite NAPQL, the generated metabolites in the present work showed less reactivity. However, a more precise assessment can only be made in combination with a quantification of oxidation products, for example by means of ICP-MS.

This work demonstrates that this purely instrumental approach is capable of simulating metabolite-protein adduct formation and to assess the reactivity of formed metabolites fast and easily. This is especially true for electrophilic species like quinoid metabolites, which can be generated during

the oxidative phase I metabolism in the liver and through dehydrogenation reactions out of catechols in the electrochemical approach.

Acknowledgement The German Federal Environmental Foundation (Deutsche Bundesstiftung Umwelt, DBU, Osnabrück, Germany) is gratefully acknowledged for financial support in form of a Ph.D. scholarship for Helene Faber.

References

1. Helfgott SM, Sandberg-Cook J, Zakim D, Nestler J (1990) *JAMA* 264:2660–2662
2. Stierlin J, Faigle W (1979) *Xenobiotica* 9:611–621
3. Tang W (2003) *Curr Drug Metab* 4:319–329
4. Pumford NR, Myers TG, Davila JC, Highet RJ, Pohl LR (1993) *Chem Res Toxicol* 6:147–150
5. Hargus SJ, Amouzedeh HR, Pumford NR, Myers TG, McCoy SC, Pohl LR (1994) *Chem Res Toxicol* 7:575–582
6. Shen S, Hargus SJ, Martin BM, Pohl LR (1997) *Chem Res Toxicol* 10:420–423
7. Shen S, Marchick MR, Davis MR, Doss GA, Pohl LR (1999) *Chem Res Toxicol* 12:214–222
8. Bort R, Macé K, Boobis A, Gómez-Lechón MJ, Pfeifer A, Castell J (1999) *Biochem Pharmacol* 58:787–796
9. Jurima-Romet M, Crawford K, Huang HS (1994) *Toxicol In Vitro* 8:55–66
10. Kretz-Rommel A, Boelsterli UA (1993) *Toxicol Appl Pharmacol* 120:155–161
11. Zhou S (2003) *J Chromatogr B Analyt Technol Biomed Life Sci* 797:63–90
12. Jurva U, Wikstrom HV, Weidolf L, Bruins AP (2003) *Rapid Commun Mass Spectrom* 17:800–810
13. Lohmann W, Baumann A, Karst U (2010) *LC GC Europe* 23:1–7
14. Nouri-Nigeh E, Bischoff R, Bruins AP, Permentier HP (2011) *Curr Drug Metab* 12:359–371
15. Baumann A, Karst U (2010) *Expert Opin Drug Metab Toxicol* 6:715–731
16. Permentier HP, Bruins AP, Bischoff R (2008) *Mini Rev Med Chem* 8:46–56
17. Zettersten C, Lomoth R, Hammarström L, Sjöberg PJR, Nyholm L (2006) *J Electroanal Chem* 590:90–99
18. Lohmann W, Hayen H, Karst U (2008) *Anal Chem* 80:9714–9719
19. Madsen KG, Skonberg C, Jurva U, Cornett C, Hansen SH, Johansen TN, Olsen J (2008) *Chem Res Toxicol* 21:1107–1119
20. Torii S, Tanaka H (2001) In: Hammerich O, Lund H (eds) *Organic electrochemistry*, 4th edn. Marcel Dekker, New York
21. Madsen KG, Olsen J, Skonberg C, Hansen SH, Jurva U (2007) *Chem Res Toxicol* 20:821–831
22. Baumann A, Lohmann W, Schubert B, Oberacher H, Karst U (2009) *J Chromatogr A* 1216:3192–3198
23. Tang W, Stearns RA, Wang RW, Chiu SH, Baillie TA (1999) *Chem Res Toxicol* 12:192–199
24. Dieckhaus CM, Fernandez-Metzler CL, King R, Krolikowski PH, Baillie TA (2005) *Chem Res Toxicol* 18:630–638